

Supporting Information

1. SI - Models

Species state models

We used multi-species meta-community models in this study following the abundance-based Dorazio/Royle/Yamaura (DRY) model (Yamaura et al. 2012) for trees and incidence-based Dorazio/Royle (DR) model (Dorazio and Royle 2005) for mammals.

The unobserved latent states of species k at site i for tree count (N_{ik}) (z_{ik}) were modelled as a Poisson distribution with expected abundance (λ_k). Mammals state was modelled using mammal incidence and Bernoulli trial with the expected probability of occupancy (Ψ_k) (Table 1). The observed tree counts (Y) and total number of mammal incidences (Y_{sum}) were both simulated as Binomial trials with a probability which is the product of the species occurrence (λ_k for trees and Ψ_k for mammals) and detection probabilities (p_k).

For trees, we assumed that all tree species have equal and perfect probability of detection. We therefore included the occurrence data of trees without any replication and modelled the Landscape scale unit (LSU) level variation in abundance per tree species. We modelled tree counts following the Dorazio/Royle/Yamaura (DRY) model (Yamaura et al. 2012). To estimate occupancy of mammal species we used the Dorazio/Royle (DR) community occupancy model (Dorazio et al. 2006; Dorazio and Royle 2005) where we took into account heterogeneity in detection by undertaking temporally replicated camera trap surveys within each camera trap grid.

SI Table 1: Details of the hierarchical occurrence models accounting for detection for the trees and mammals

Taxonomic group:	Trees	Mammals
State process: occurrence	$N_{ik} \sim \text{Poisson}(\lambda_k)$	$z_{ik} \sim \text{Bernoulli}(\Psi_k)$
Observation process: detection	$Y_{ik} N_{ik} \sim \text{Binomial}(N_{ik}, p_{ik})$	$Y_{sum_{ik}} z_{ik} \sim \text{Binomial}(J_i, z_{ik} p_{ijk})$
Models of species heterogeneity in occurrence	Model: $\log(\lambda_{ik}) = \beta_{0k} + \beta_{1k} * \text{LDI} + \beta_{2k} * \text{LDI}^2 + \beta_{3k} * \text{ME}_{\text{resid}} + \beta_{4k} * \text{HL}_{\text{resid}} + \beta_{5k} * \text{MAP}$ <i>LDI = Land Division Index</i> <i>ME = Proportion of miombo extent i.e. miombo woodland at 1km scale.</i>	Model: $\log(\lambda_{ik}) = \beta_{0k} + \beta_{1k} * \text{LDI} + \beta_{2k} * \text{LDI}^2 + \beta_{3k} * \text{LDI}^3 + \beta_{4k} * \text{ME}_{\text{resid}} + \beta_{5k} * \text{HL}_{\text{resid}} + \beta_{6k} * \text{MAP}$ <i>HL = Woody cover loss between 2010-2014</i> <i>MAP = Mean Annual Precipitation</i>
Detection heterogeneity	$\text{logit}(p_{ik}) = \alpha_{0k}$	$\text{logit}(p_{ijk}) = \alpha_{0k}$
Species-specific effects	$\beta_{jk} \sim \text{Normal}(\mu_{\beta j}, \sigma^2_{\beta j})$	

k index of species of trees and mammals

ME_{resid} and HL_{resid} refer to the residuals of “ $ME \sim LDI$ ”, “ $HL \sim LDI + ME_{resid}$ ”, respectively.

For both, detection and occurrence, the species-specific parameters were constrained and drawn from a common normal prior distribution. Therefore, treating the species-specific effects as random and relying on the assumption that species-specific effects are stochastic and exchangeable – “*similar although not identical*” (Kéry and Royle 2016; Kéry and Schaub 2012). Hence, models here are effectively multilevel mixed-effects hierarchical models.

Community state

From the output of the species-state models, we computed two community-state parameters: (i) species richness (SR), and (ii) mean community dissimilarity (MCD) – a measure of variation in community composition, or β -diversity. The MCD is equivalent to the Local Contribution to β -Diversity (LCBD) of Legendre & De Cáceres (2013). Communities can change in species composition due to two processes: (i) replacement of species and thereby turnover in the community, and (ii) loss of species with low or no turnover and thereby nestedness in the community. We computed both the turnover and the nestedness components of the multi-part Sorenson dissimilarity, after Baselga (2010).

The community state parameters were estimated as posterior means within the community occurrence model framework using the detection-corrected matrix of species occurrence. The c^{th} community parameter at site i , A_{ic} derived from the posterior distribution is not independent and is based upon interrelated estimates: the posterior mean (μ_{ic}) and standard deviation (σ^2_{ic}). We modelled the posterior mean estimates as a function of the land cover variables in linear additive combination and propagated the estimation uncertainty (i.e. the standard deviation) by constructing two residual components - known standard deviation and residual error, ϵ_c .

SI Table 2: Details of the detection corrected community-level models for trees and mammals

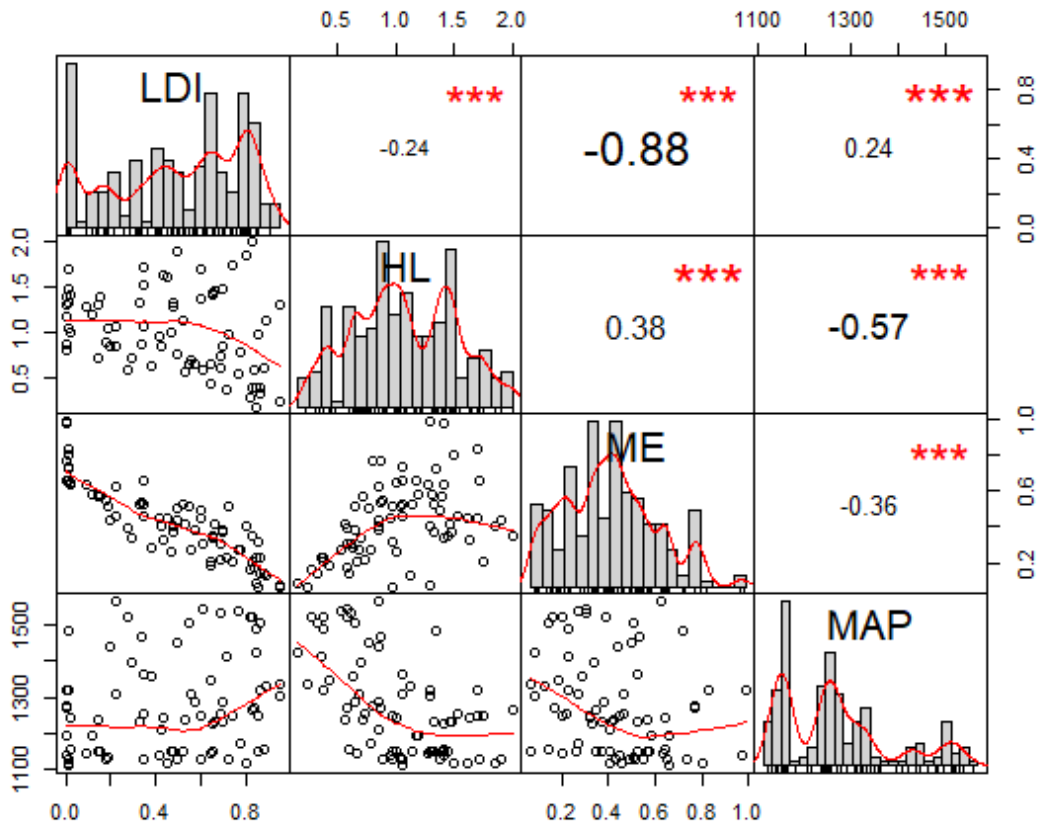
Community parameters	$A_{ic} \sim Normal(\mu_{ic}, \sigma^2_{ic})$
Models of community mean estimates	<p>Model for mammal diversity: $\mu_{ic} = \beta_{0k} + \beta_{1k} * LDI + \beta_{2k} * LDI^2 + \beta_{3k} * LDI^3 + \beta_{4k} * ME_{resid} + \beta_{5k} * HL_{resid} + \beta_{6k} * MAP + \epsilon_c$</p> <p>Model for Tree diversity: $\mu_{ic} = \beta_{0k} + \beta_{1k} * LDI + \beta_{2k} * LDI^2 + \beta_{3k} * ME_{resid} + \beta_{4k} * HL_{resid} + \beta_{5k} * MAP + \epsilon_c$</p>

2. Details of fragmentation metrics

A number of fragmentation metrics (or indices) such as number of patches, nearest neighbor distance, splitting index, fractal index, effective mesh size (EMS), splitting index, etc. have been proposed and used in several studies (Hill and Caswell 1999; Jaeger 2000; MacLean and Congalton 2015; Magrath et al. 2014). However, these metrics often describe similar processes,

are interrelated and often are partially or wholly redundant inherently or empirically (Mcgarigal 2015). We used the proportion of woodland instead of mean patch size as it is a more direct way of representing the quantity of habitat in the landscape. Jaeger (2000), after comparing various indices of fragmentation, concluded that EMS was most suitable for comparing fragmentation among landscapes with varying habitat quantities. However, in the landscapes we studied, EMS was highly correlated with LDI ($R^2=0.86$ for mammal grids, $R^2=0.83$ for tree grids). We used LDI because its simplicity should make it more intuitive.

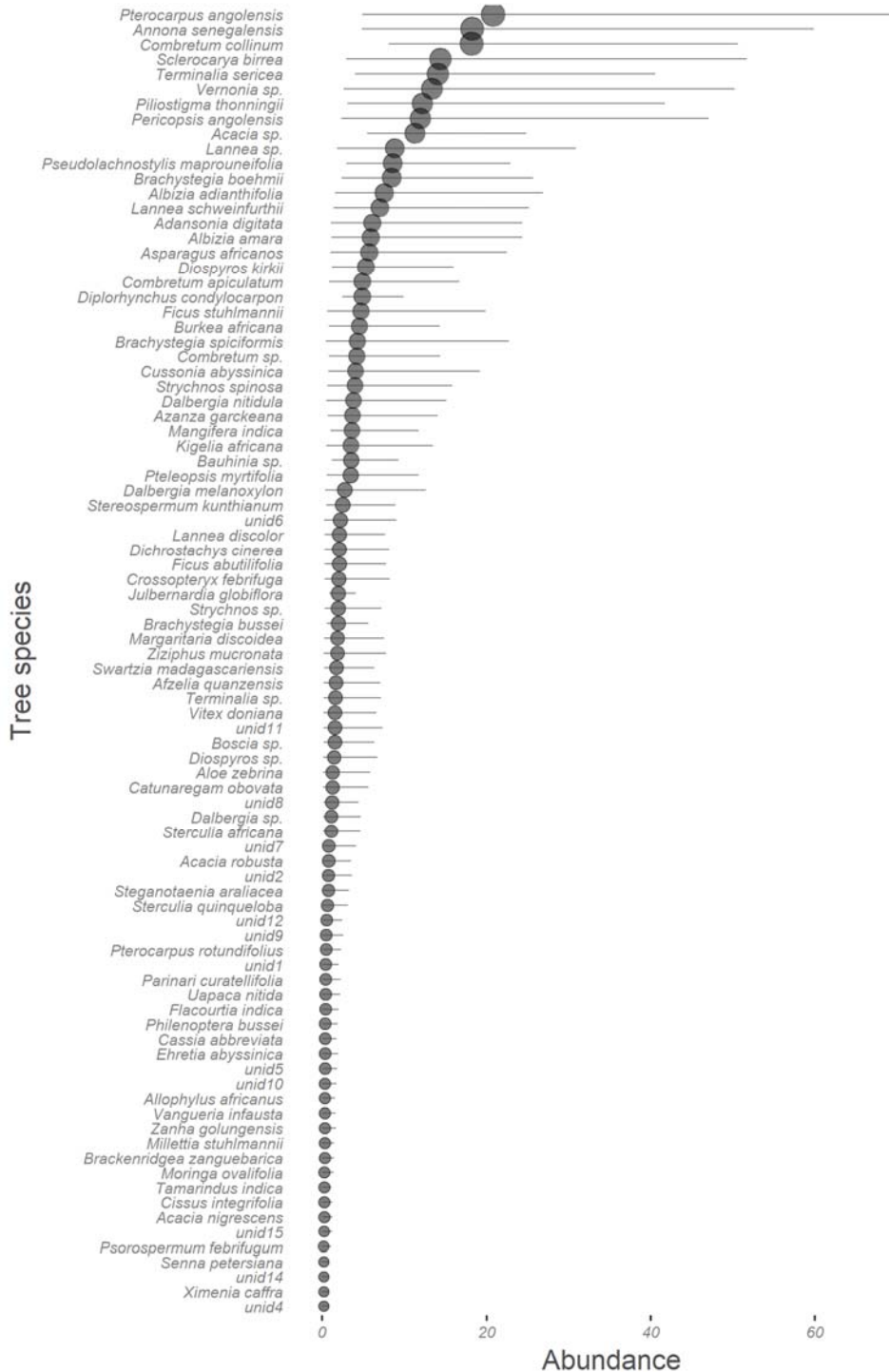
Also, LDI was correlated with ME (woodland cover) and HL (intensity of woodland loss) (SI-Figure 1). To reduce multicollinearity, we decided to use residuals of ME and HL following the method of sequential regression in the order LDI + ME + HL



SI Figure 1: Correlation between predictors

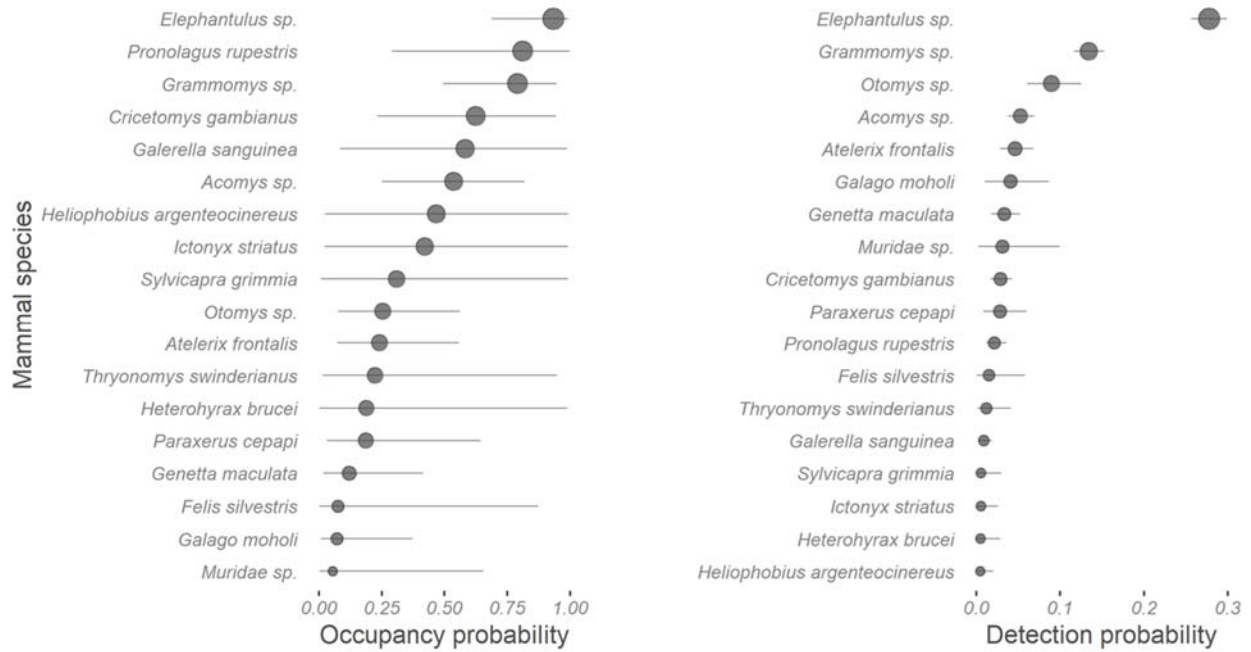
3. Average occupancy of mammals and abundance of trees

Tree species



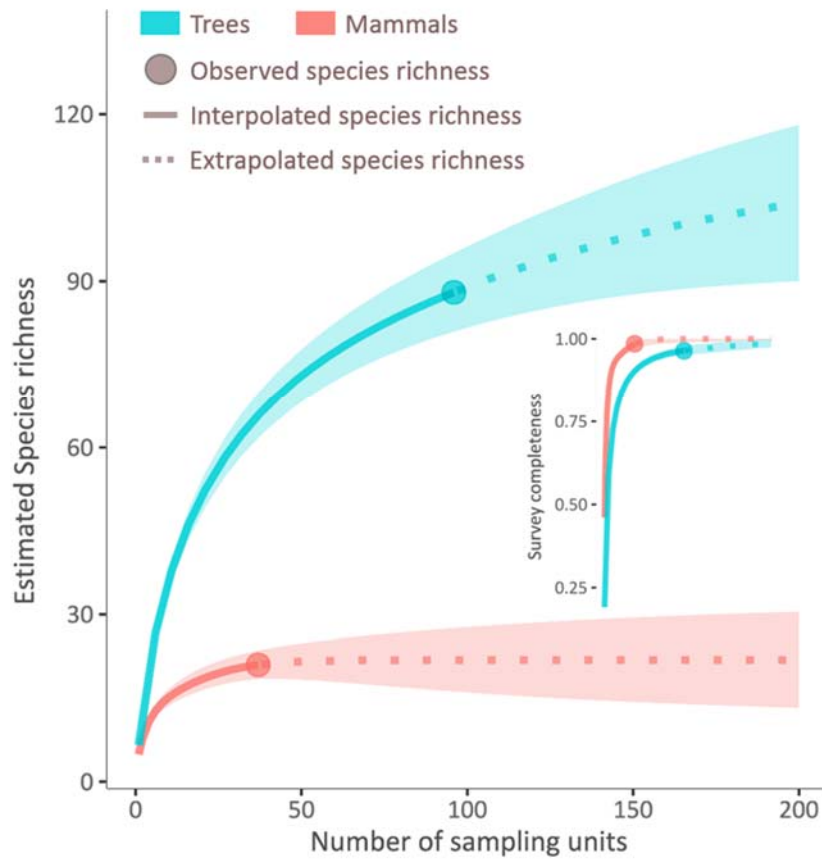
SI-Figure 3: Tree species found in the study area ordered by abundance, indicating dominance of non-miombo species in the region. The top 12 most abundant species accounted for over 50% of all trees observed during the study. *Brachystegia boehmii* and *Julbernardia globiflora* are representative of miombo in the top 12 species.

Mammal species



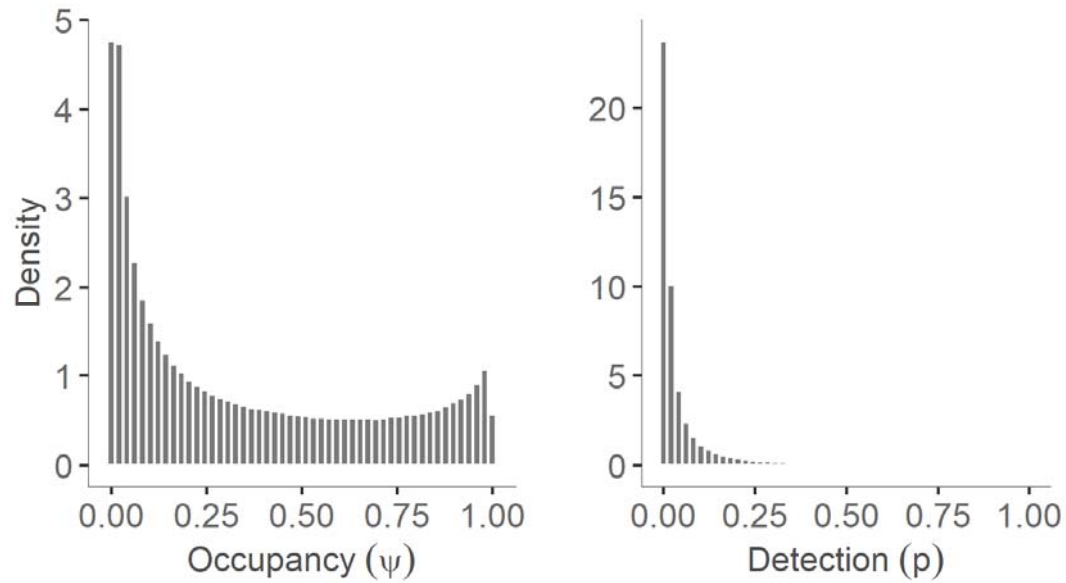
SI-Figure 2: Occupancy and detection probabilities of mammal species at the scale of 1 km² during early dry season (April-July) 2016. The mammal communities in the miombo-agricultural landscape are dominated by the elephant shrew (*Elephantulus sp.*), murids (such as *Grammomys sp.* and *Acomys sp.*) and the rock hare (*Pronolagus rupestris*). Mongooses (*Galerella sanguinea*) and genets (*Genetta maculata*) are the dominant predators in this system. In both, the occupancy and detection plots, species are arranged in decreasing order of occupancy (also indicated by the size of the circle).

4. Species accumulation and survey completeness



SI-Figure 4: The sample rarefaction- and extrapolation-based species richness estimate and accumulation curve with 95% confidence interval (the shaded region) shows species asymptote and survey completeness (>0.97), indicating that our study covered most of the species found in the region for both taxonomic groups (trees and mammals). The detection-corrected species richness estimates from the hierarchical models were higher than the above-shown sample-based estimates.

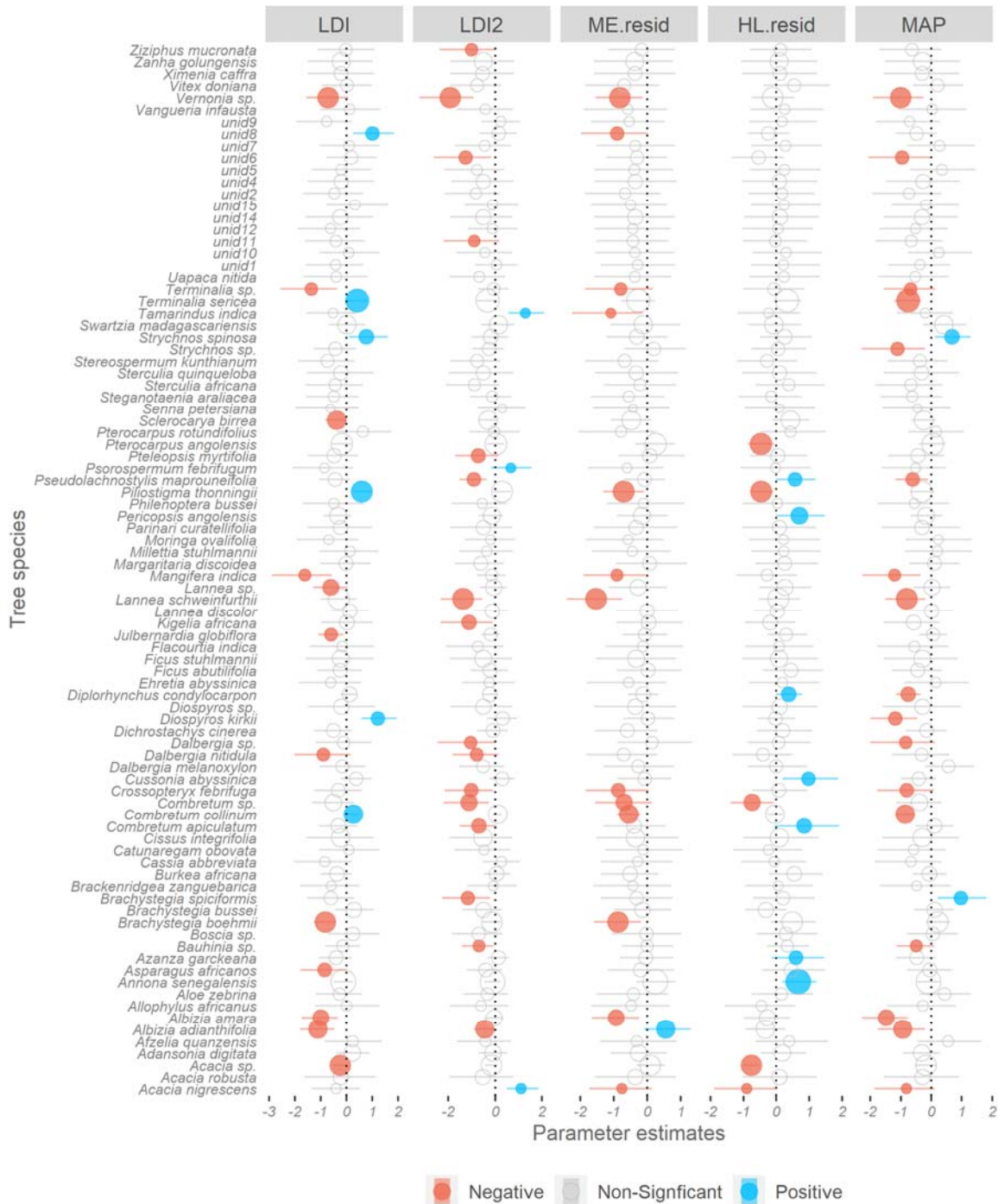
5. Occupancy and detection variability in mammals



SI-Figure 5: Distribution of community level average occupancy (μ) and detection probability ($p\mu$) between mammal species based on parameters from the hierarchical occurrence model (μ , s^2 , $p\mu$, ps^2) for the scale of km^2 and single season survey (April-July) in 2016.

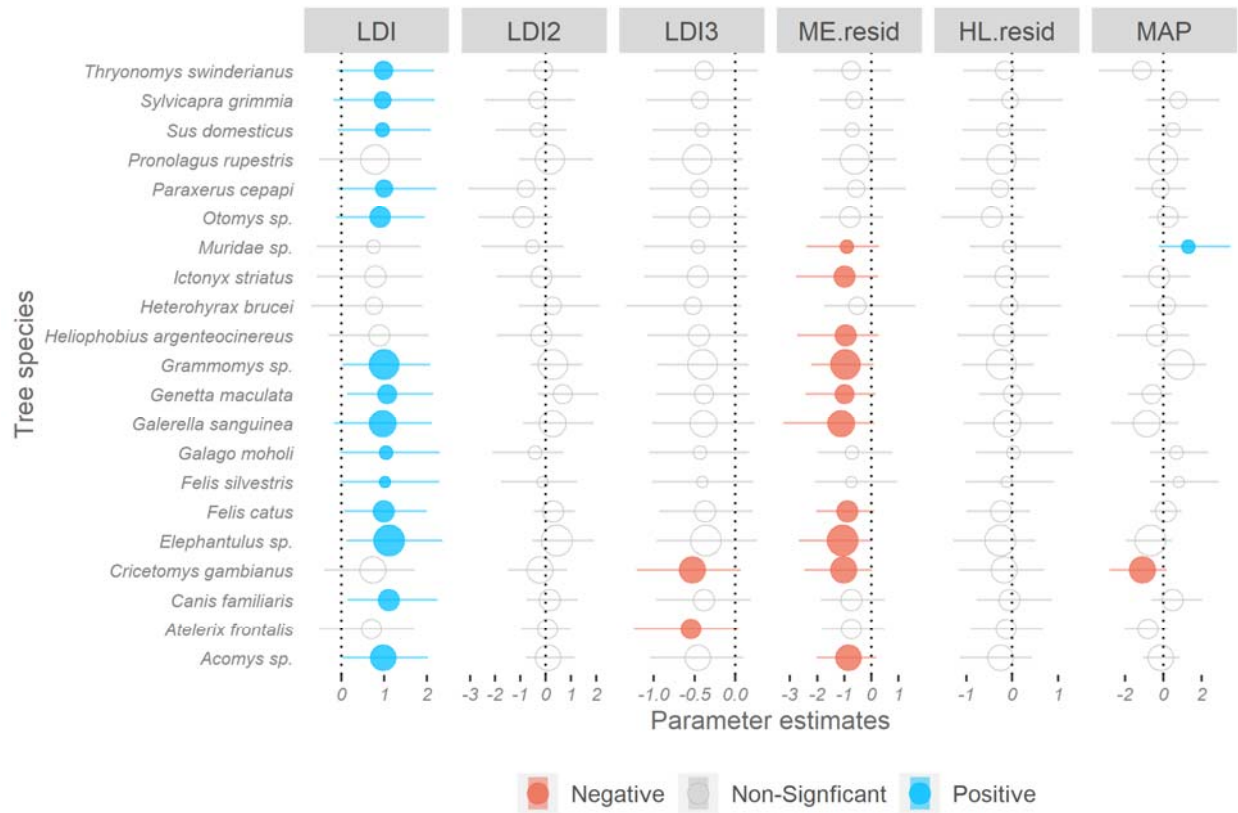
6. Coefficient plots of occurrence models.

Tree species



SI- Figure 6: The coefficient plot of tree species' responses to the landscape division index shows a largely negative effect of LDI on species abundance. The positions of the circles represent β -coefficients, the size of the circles indicates intercept (the mean abundance of species across the study area), horizontal lines on the circles show 95% CI, and colours signify the direction of the effect.

Mammal species



SI- Figure 7: Response of mammals to landcover variables. Models of mammal species occupancy to examine their response to landscape division index (LDI), suggest a possible nonlinear effect of LDI, since species increase (in blue circles) with LDI and decrease (orange circles) at LDI3. LDI was associated with increase in occupancy of elephant shrews, murids (African spiny mouse, *Acomys sp.*, and thicket rat, *Grammomys sp.*) which are known to survive in human disturbed landscapes. Further, species such as the African giant rat (*Cricetomys gambianus*) and South African hedgehog (*Atelerix frontalis*), and Spiny mouse (*Acomys*) reduced with LDI3. The positions of the circles represent β - coefficients, the size of the circles indicate the probability of occupancy of the species across the study area, the horizontal lines on the circles show 95% CI, and colours signify the direction of the effect.